Original Article

Clinical utility of combined T2-weighted imaging and T2-mapping in the detection of prostate cancer: a multi-observer study

Chau Hung Lee[1,2], Matthias Taupitz[1], Patrick Asbach[1], Julian Lenk[1], Matthias Haas[1]

[1]Department of Radiology, Charite-Universitätsmedizin Berlin, Campus Benjamin Franklin, Corporate Member of Freie Universität Berlin, Humboldt-Universität zu Berlin, and Berlin Institute of Health, Berlin, Germany; [2]Department of Radiology, Tan Tock Seng Hospital, Singapore, Singapore

Correspondence to: Patrick Asbach. Department of Radiology, Charite-Universitätsmedizin Berlin, Campus Benjamin Franklin, Corporate Member of Freie Universität Berlin, Humboldt-Universität zu Berlin, and Berlin Institute of Health, Hindenburgdamm 30, 12203 Berlin, Germany. Email: patrick.asbach@charite.de.

Background: To evaluate the clinical utility of combined T2-weighted imaging and T2-mapping for the detection of prostate cancer.

Methods: Forty patients underwent multiparametric magnetic resonance imaging (mpMRI) and T2-mapping of the prostate. Three readers each reviewed two sets of images: T2-weighted fast spin-echo (FSE) sequence (standard T2), and standard T2 in combination with T2-mapping. Each reader assigned probability scores for malignancy to each zone [peripheral zone (PZ) or transition zone (TZ)]. Inter-observer variability for standard T2 and combined standard T2 with T2-mapping were assessed. Diagnostic accuracy was compared between standard T2 and combined standard T2 with T2-mapping.

Results: There was fair agreement between all three readers for standard T2 [intraclass correlation coefficient (ICC) =0.56] and combined standard T2 with T2-mapping (ICC =0.58). There was no significant difference in the area under the receiver operator characteristics curve for standard T2 compared to combined standard T2 with T2-mapping (0.89 *vs.* 0.82, P=0.31). Sensitivity (Sn) for combined standard T2 with T2-mapping was significantly higher compared to standard T2 alone (73.0% *vs.* 49.2%, P=0.006). Specificity (Sp) for combined standard T2 with T2-mapping was borderline significantly lower compared to standard T2 alone (89.3% *vs.* 94.9%, P=0.05). There was no significant differences between the negative predictive values (NPVs) and positive predictive values (PPVs) (P=0.07, P=0.45).

Conclusions: Combination of T2-weighted imaging and T2-mapping could potentially increase Sn for prostate malignancy compared to T2-weighted imaging alone.

Keywords: Prostate; magnetic resonance imaging (MRI); T2-mapping

Submitted Feb 10, 2020. Accepted for publication Jun 09, 2020.
doi: 10.21037/qims-20-222
View this article at: http://dx.doi.org/10.21037/qims-20-222

Introduction

Multiparametric magnetic resonance imaging (mpMRI) of the prostate is an established imaging technique for the detection of prostate cancer (1). It utilizes T2-weighted imaging, diffusion-weighted imaging (DWI) and dynamic contrast-enhanced (DCE) imaging to stratify the probability of prostate cancer, in accordance to PI-RADS (2). mpMRI has been shown to improve the detection of clinically significant cancer while reducing the detection of insignificant cancers compared to standard systematic transrectal ultrasound-guided biopsy (3,4). By identifying the most suspicious areas within the prostate, targeted biopsy can be performed, thus potentially reducing the number of biopsy cores and accompanying morbidity (5,6).

However, studies have shown significant overlap of DWI

and DCE imaging findings between malignancy and benign conditions such as prostatitis and stromal hyperplasia (7,8). Development of newer quantitative imaging techniques such as intravoxel incoherent motion (IVIM), diffusion tensor imaging (DTI) and diffusion kurtosis imaging (DKI), allow quantitative assessment and show potential in improving cancer detection and predicting tumor aggressiveness (9-11).

T2-mapping using MRI is a quantitative technique where basically the T2-relaxation times of tissues can be derived from a series of T2-weighted spin-echo sequences or from the echoes of a spin-echo multi-echo sequence and then be encoded, for example, into a color map (12). This technique provides functional information in terms of the different sizes of the water compartments as well as the different proportions of stromal and glandular tissue between normal and malignant prostatic tissue, to complement anatomical and spatial information provided by standard T2-weighted imaging (13). T2-mapping is well-established for evaluation of brain and cardiac tissue as well as changes in hyaline cartilage (14-16). Preliminary studies have also shown that T2-mapping can be useful in differentiating prostate malignancy from benign prostatic tissue based on differences in T2-relaxation times (17,18). One study in particular proposed a threshold T2-relaxation time of 99 ms to achieve a 92% sensitivity (Sn) and 97% specificity (Sp) for cancer detection in the peripheral zone (PZ) (19). However, the addition of a mapping sequence increases the overall prostate MR protocol acquisition time. This might be compensated by a mapping sequence that allows the reconstruction of a simulated T2-weighted image that could be used instead of the standard T2-weighted image.

We aim to evaluate the clinical utility of combined T2-weighted imaging and T2-mapping for the detection of prostate cancer.

Methods

Patient cohort

This prospective single-center study was approved by the institutional board of Charité University Hospital—Campus Benjamin Franklin (No. EA4/010/16) and informed consent was taken from all the patients.

Subjects were recruited between December 2016 and May 2018. Prostate MRI was clinically indicated in all subjects and requested by a referring doctor. Inclusion criteria were: (I) clinical suspicion for prostate cancer based on either a raised serum prostate-specific antigen (PSA) defined as above 4 ng/mL at our institution, a palpable nodule on digital rectal examination, a suspicious finding on trans-rectal ultrasound or a combination thereof and (II) no histologically-proven prostate cancer (Gleason score ≥6) at time of MRI. Exclusion criteria were: (I) contraindications to intravenous gadolinium-based contrast, for example moderate renal impairment (eGFR <60 mL/min/1.73 m^2) or allergy, (II) MRI-incompatible implants, (III) prior prostate biopsy, (IV) treatment for prostate cancer or systemic therapy for benign prostatic hypertrophy (BPH), (V) the inability to complete the full MRI study, for example due to claustrophobia or physical handicap, (VI) imaging artefacts that significantly degraded image quality. All included subjects provided written informed consent prior to the MRI scan. Patients who met all inclusion and exclusion criteria were screened consecutively. Forty-one patients were enrolled and gave written informed consent for this study. One patient could not complete the MRI scan due to claustrophobia. No patients were excluded due to poor MRI image quality. Forty patients completed the MRI scans and were included as final cohort in this study. A total of 80 prostatic zones [40 PZ, 40 transition zone (TZ)] were analyzed. Mean patient age was 70.3 (range, 57 to 84) years. Biopsy results were available in 14 out of 40 patients, either from systematic or targeted biopsies, performed after the MRI scan. Prostate malignancy was subsequently confirmed by biopsy in 11 patients (Gleason 6=1 patient, Gleason 7=6 patients, Gleason 8=4 patients). Three patients had negative biopsy results.

Imaging technique

All scans were performed on a 3 Tesla MR scanner (Magnetom Skyra, Siemens Healthineers, Erlangen, Germany) using body phased-array receiver coil (18-channel, 3 rows of 6 elements each) with an integrated spine-array receiver coil (32-channel, 8 rows of 4 elements each).

T2-mapping of the whole prostate was performed using a vendor provided works-in-progress model-based accelerated T2-mapping multi-echo sequence technique, in the axial plane (20). Standard small field-of-view (FOV) axial, sagittal and coronal T2-weighted fast spin-echo (FSE) images were also acquired for comparison, as per routine MRI protocol. The T2-mapping and T2-weighted FSE scan parameters are summarized in *Table 1*. In addition, the color-coded parametric T2-maps for each scan were derived using evaluation software.

Table 1 T2-weighted imaging and T2-mapping scan parameters

Scan parameter	T2-weighted FSE	T2-mapping
TR (ms)	4,040	4,820
TE (ms)	116	Measured: 10.8–172.8 (10.8 ms intervals); simulated: 50, 100, 116, 130, 150
Turbo factor	25	–
Flip angle (degrees)	160	180
In-plane resolution (mm)	0.52×0.47	0.75×0.56
Slice thickness (mm)	3 (no gap)	3 (no gap)
FOV (mm)	180	180
Acceleration factor (GRAPPA)	2	2
Bandwidth (Hz/pixel)	200	220
Scan time	3 min 56 s	3 min 58 s

FSE, fast spin-echo; TR, repetition time; TE, echo time; FOV, field-of-view.

The other MRI sequences acquired were: axial DWI (with acquired b values of 0, 50, 500, 1,000 s/mm^2, and calculated b value: 1,400 s/mm^2), large FOV axial T1-weighted spin-echo sequence of the whole pelvis and DCE imaging. The DWI and DCE imaging sequences were used for assessing prostate changes according to PI-RADS version 2, with the aim of generating the reference standard for each case, while the T1-weighted sequence was used to assess for hemorrhage. The DWI, DCE and T1-weighted images otherwise were not subjected to investigation in this study.

Image analysis

The prostate was divided into the PZ and the TZ, based on the standard T2-weighted FSE sequence. The central zone was considered part of the TZ in this study.

Three readers of varying experience in prostate MRI, R1 (a final year radiology resident), R2 (a junior radiology consultant with 5 years of experience with prostate MRI) and R3 (a senior radiology consultant with 15 years of experience with prostate MRI) separately reviewed two sets of images for each patient: (I) axial T2-weighted FSE sequence (standard T2) and (II) T2-mapping with reconstructed color-coded parametric T2-map. Since T2-mapping was derived from axial T2-weighted images, the readers were only required to review the standard T2 images in the axial plane. To allow a uniform standardized comparison, the sagittal and coronal T2-weighted, DWI, DCE and T1-weighted images were not made available to readers for review. The readers were also blinded to histological findings. The reading was conducted in two sessions 1 week apart, to avoid recall bias.

The first reading session involved reviewing the standard T2 images. First, a T2 PI-RADS score of 1 to 5 was assigned to the most suspicious lesion in each prostatic zone based on PI-RADS version 2 guidelines (21). If there was no focal lesion, a T2 PI-RADS score of 1 was assigned (normal). This score was modified to reflect the probability of clinically significant prostate malignancy on a Likert-like scale (*Table 2*).

In the second reading session, the standard T2 and the parametric T2-maps were reviewed in combination and the most suspicious lesion in each prostatic zone was again assigned a probability score for clinically significant cancer based on a Likert-like scale (*Table 2*). This was performed qualitatively by evaluating the morphology on the standard T2, and quantitatively using the parametric T2-maps by applying a threshold T2-relaxation time of 99 ms below which the suspicion of malignancy is increased (19). During quantitative assessment using the parametric T2-maps, a region of interest (ROI) in each zone was marked with a circular marker and the mean T2-relaxation time within the ROI was recorded. The T1-weighted sequence was also evaluated to avoid areas of hemorrhage or calcification while marking the ROI.

Reference standard

As not all patients had histological correlation available, the PI-RADS score in each zone was taken as reference standard,

Table 2 Scoring scale for probability of prostate malignancy in each zone

T2 PI-RADS score (for standard T2)	Likert-like score (for simulated T2 and combined standard T2 with T2-mapping)	Probability of clinically significant prostate malignancy
1	1	Very low
2	2	Low
3	3	Intermediate
4	4	High
5	5	Very high

taking into account DWI and DCE imaging as well ("overall PI-RADS score"). This score was assigned in consensus by two expert observers (with combined 25 years of prostate MRI experience) not involved in the readings. The full MRI study (including axial, coronal and sagittal T2-weighted, DWI and DCE imaging) were available for review by the two expert observers. In our study, an overall PI-RADS score of 1–3 was considered reference standard negative while an overall PI-RADS score of 4 and 5 was considered reference standard positive for malignancy (22,23).

Statistical analysis

Inter-observer agreement between three readers for standard T2 and combined standard T2 with T2-mapping was calculated using the intraclass correlation coefficient (ICC) for more than two observers.

The T2 PI-RADS scores for standard T2 and the Likert scores for combined standard T2 with T2-mapping were compared using the area under the receiver operating characteristic curve (AUROC).

Point estimates for Sn, Sp, positive predictive values (PPVs) and negative predictive values (NPVs) were derived by constructing the 2×2 contingency table. Diagnostic performance in terms of Sn, Sp, PPV and NPV for standard T2 alone and combined standard T2 with T2-mapping were compared using the McNemar Test for paired observations.

In a subgroup analysis, for each zone assigned a particular T2 PI-RADS score, the diagnostic accuracy of standard T2 alone and combined standard T2 with T2-mapping was compared using the McNemar Chi-Square test.

For purposes of statistical analysis, a reader-assigned T2 PI-RADS or Likert scale score of 1 to 3 was considered as scan-negative while a score of 4 to 5 was considered scan-positive for malignancy.

Individual reader and overall results are presented with 95% confidence intervals (CIs) and P values. Significance level for all comparisons was set at 5%. Statistical analysis was performed using SPSS Statistics for Windows, version 21.0 (IBM Corp., Armonk, NY, USA).

Results

The probability scores assigned by each reader as well as the overall PI-RADS scores (reference standard) assigned in consensus by two expert observers, with their distribution across the PZs and TZs, are summarized in *Table 3*.

There was fair agreement between all three readers for standard T2 (ICC =0.56) and combined standard T2 with T2-mapping (ICC =0.58).

The overall AUROC (*Figure 1*) was also higher for combined standard T2 with T2-mapping, but this was not statistically significant (0.89 *vs.* 0.82, P=0.31).

The combined Sn for all readers was significantly higher for combined standard T2 with T2-mapping compared to standard T2 alone (73.0% *vs.* 49.2%, P=0.006) in the detection of prostate cancer. The combined NPV was also higher for combined standard T2 with T2-mapping, approaching statistical significance (90.3% *vs.* 84.9%, P=0.07). However combined Sp was borderline significantly lower for combined standard T2 with T2-mapping compared to standard T2 alone (89.3% *vs.* 94.9%, P=0.05). There was no significant difference between the combined PPV (P=0.45). These results are summarized in *Table 4*.

In a subgroup analysis, the T2 PI-RADS score assigned on standard T2 in the first reading session was compared to the corresponding Likert score assigned for combined standard T2 with T2-mapping in the second reading session, for each zone. This was performed to assess if there was a subgroup where the addition of T2-mapping to T2-weighted imaging would be particularly useful. This analysis showed that the addition of T2-mapping significantly

Table 3 Probability scores (based on Table 2) assigned by each reader and the overall PI-RADS score assigned in consensus by two expert observers (as reference standard), with their distribution in the PZ and TZ

Reader	Probability scores for clinically significant prostate cancer	PZ				TZ			
		2	3	4	5	2	3	4	5
Reader 1	Standard T2	14	10	10	6	23	8	3	6
	Standard T2 + T2 map	13	8	13	6	22	7	6	5
Reader 2	Standard T2	12	11	16	1	26	11	1	2
	Standard T2 + T2 map	14	7	9	10	31	8	0	1
Reader 3	Standard T2	14	15	6	5	24	13	0	3
	Standard T2 + T2 map	22	6	7	5	32	5	1	2
Reference standard	–	23	2	8	7	33	1	0	6

PZ, peripheral zone; TZ, transition zone.

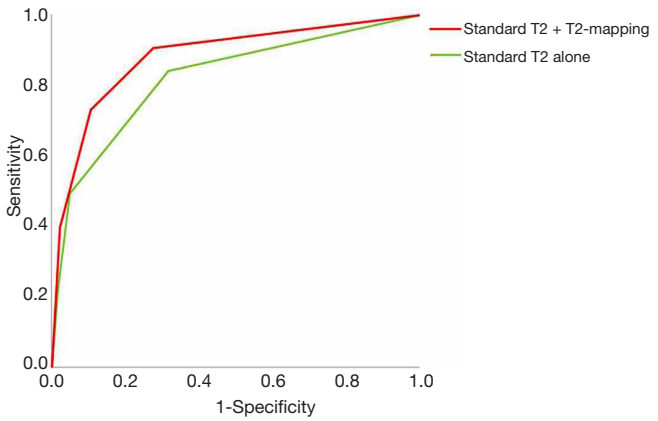

Figure 1 Overall receiver operating characteristic curves for combined T2-weighted imaging with T2-map and T2-weighted imaging alone.

increased the diagnostic accuracy compared to standard T2 alone, for zones assigned a T2 PI-RADS score of 3 (79.7% for combined standard T2 with T2-mapping *vs.* 63.8% for standard T2 alone, P=0.04). For zones assigned T2 PI-RADS scores of 2, 4 or 5, the addition of T2-mapping did not significantly improve diagnostic accuracy. These results are summarized in *Table 5*.

TZs assigned with a T2 PI-RADS score of 3 were further reviewed. Across all three readers, there were 31 zones assigned a T2 PI-RADS score of 3. The addition of T2-mapping correctly "downgraded" the probability scores in 13 zones to a "low probability of clinically significant prostate cancer" (Likert-like score 2) whilst correctly "upgraded" the probability scores in two zones to a "high or very high probability of clinically significant

Table 4 Comparison of the combined diagnostic performance for T2-weighted imaging alone and in combination with T2-mapping

Statistical parameter	Standard T2 alone	Combined standard T2 with T2-mapping	P value
AUROC (95% CI)	0.82 (0.73, 0.91)	0.88 (0.81, 0.95)	0.31
Sn (95% CI), %	49.2 (36.4, 62.1)	73.0 (60.4, 83.4)	0.006*
Sp (95% CI), %	94.9 (90.6, 97.7)	89.3 (83.8, 93.4)	0.05^
PPV (95% CI), %	77.5 (63.5, 87.2)	70.8 (60.7, 79.2)	0.45
NPV (95% CI), %	84.0 (80.4, 87.0)	90.3 (86.1, 93.3)	0.07

*, combined Sn significantly higher for combined T2-weighted imaging and T2-mapping; ^, combined Sp borderline significantly lower for combined T2-weighted imaging and T2-mapping. CI, confidence interval; AUROC, area under the receiver operating characteristic curve; Sn, sensitivity; Sp, specificity; PPV, positive predictive value; NPV, negative predictive value.

Table 5 Subgroup analysis by T2 PI-RADS score

T2 PI-RADS score	Overall accuracy standard T2 alone (95% CI), %	Overall accuracy combined standard T2 with T2-mapping (95% CI), %	P value
1	–	–	–
2	92.4 (86.4, 96.3)	90.8 (84.6, 95.2)	0.66
3	63.8 (51.3, 75.0)	79.7 (68.3, 88.4)	0.04*
4	69.6 (47.1, 86.8)	69.6 (47.1, 86.8)	1
5	82.4 (56.6, 96.2)	76.5 (50.1, 93.2)	0.67

Subgroup analysis by T2 PI-RADS score, showing that combined T2-weighted imaging and T2-mapping significantly increased accuracy compared to T2-weighted imaging alone, for zones assigned a T2-PI-RADS score 3 (*). CI, confidence interval.

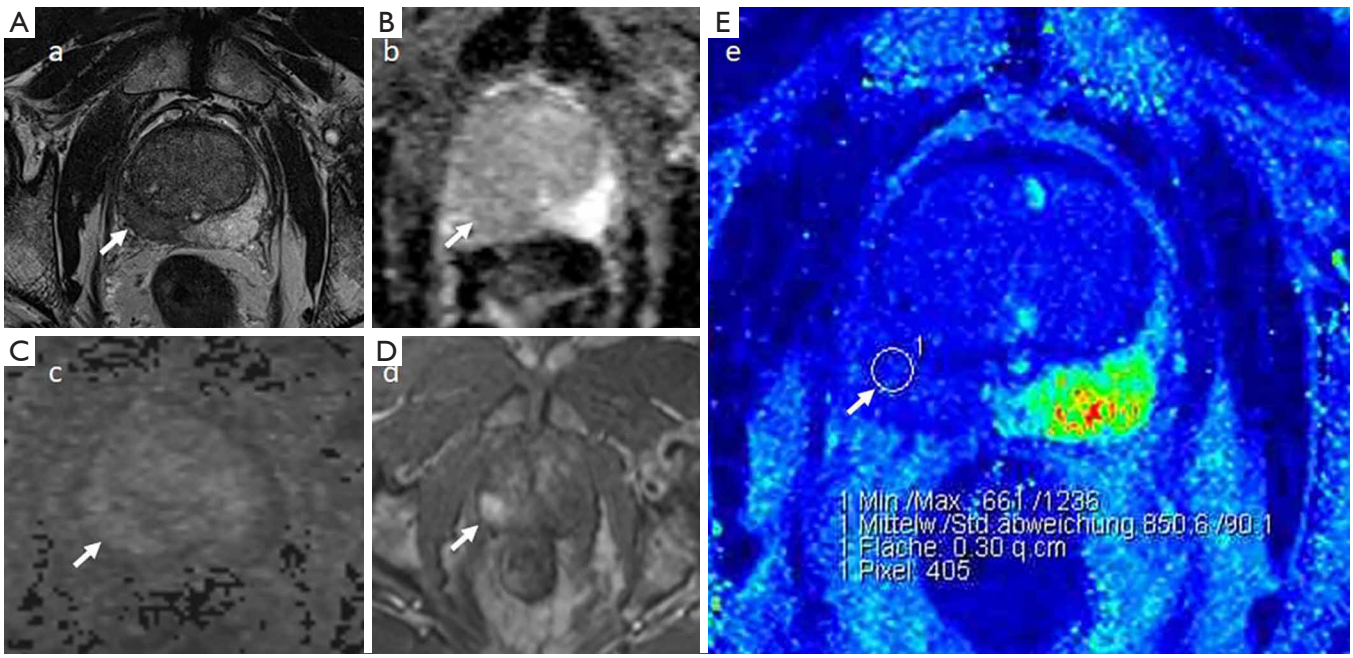

Figure 2 Prostate mpMRI of a 51-year-old gentleman with a PSA of 6.9 ng/mL. (A) T2-weighted imaging showed a focal hypointense lesion in the PZ of the right prostatic lobe (arrow); (B) ADC map also showed focal hypointensity (arrow); (C) there was corresponding mild hyperintensity on high b value DWI (b=1,400) (arrow); (D) DCE-imaging showed focal early enhancement on DCE-imaging in the PZ in the right midgland (arrow). This was given an overall PI-RADS 4 by expert consensus (reference standard positive for malignancy); (E) T2-mapping showed T2-relaxation time of 85.1 ms in the PZ at the right midgland, below threshold value of 99 ms (arrow). All three readers assigned a T2 PI-RADS score of 3 but correctly upgraded to a Likert score of 4 based on combined T2 and T2-mapping. mpMRI, multiparametric magnetic resonance imaging; PSA, prostate-specific antigen; PZ, peripheral zone; ADC, apparent diffusion coefficient; DWI, diffusion-weighted imaging; DCE, dynamic contrast-enhanced.

prostate cancer" (Likert-like score 4 or 5). There was no incorrect downgrading or upgrading of scores for this subset of zones although in the remaining 16 zones, addition of T2-mapping did not change the probability scores.

Case examples are shown (*Figures 2-4*).

Discussion

Prostate cancer detection using mpMRI, even with standardization of imaging technique, interpretation and reporting, remains subjective and dependent on reader experience (24,25). Quantitative imaging techniques are able

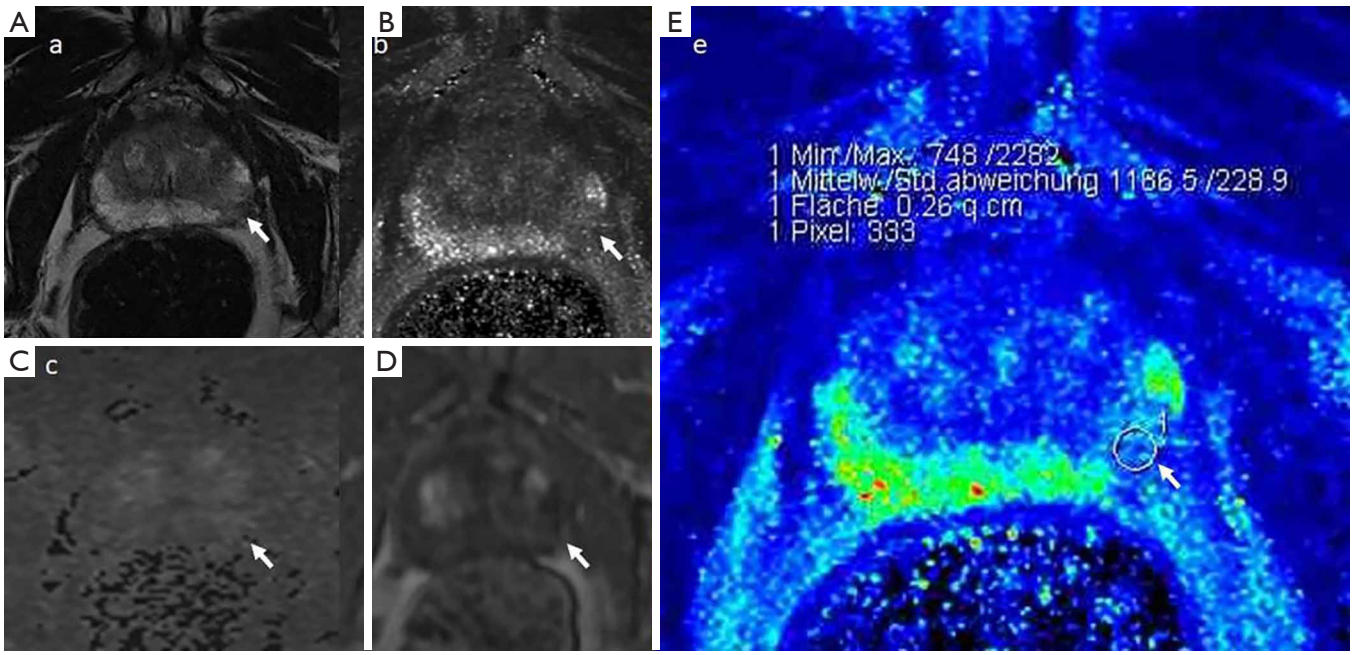

Figure 3 Prostate mpMRI of a 60-year-old gentleman with a PSA of 5.1 ng/mL. (A) T2-weighted imaging showed a focal wedge-shaped hypointensity in the PZ at the left apex (arrow); (B) ADC map showed corresponding mild focal hypointensity (arrow); (C) this was iso-intense on high b value DWI (b=1,400) (arrow); (D) DCE-imaging showed no early enhancement (arrow). The overall PI-RADS score was 2 (reference standard negative for malignancy); (E) T2-mapping showed a T2-relaxation time of 118.7 ms, above threshold value of 99 ms (arrow). This was assigned a T2 PI-RADS score of 4 by reader R2. However, this was correctly re-categorized to a Likert score of 2 based on combined T2 and T2-mapping. mpMRI, multiparametric magnetic resonance imaging; PSA, prostate-specific antigen; PZ, peripheral zone; ADC, apparent diffusion coefficient; DWI, diffusion-weighted imaging; DCE, dynamic contrast-enhanced.

to provide measurements for increased objectivity in image analysis and are increasingly being studied in the evaluation of prostate cancer (26). There is substantial literature demonstrating the usefulness of T2-relaxation times derived from quantitative T2-mapping in the detection of prostate malignancy (17,18,27,28).

In our study, we attempted to assign a single threshold T2-relaxation time in the quantitative assessment of the parametric T2-maps. However, this was challenging due to considerable overlap of T2-relaxation times between benign stromal hyperplasia and TZ malignancy (29,30). While one study proposed a cut-off T2-value of 99 ms for identifying malignancy in the PZ (19), no such cut-off could be recommended for TZ malignancy. Therefore, in our study, in addition to applying this recommended threshold T2-relaxation time while analyzing the parametric T2-maps, we also included evaluation of morphology on T2-weighted imaging, and not just assigning a probability score based on T2-relaxation times alone. We believe this should also reflect the way T2-mapping is utilized in clinical practice, and underscores the importance of assessing lesion shape and margins on T2-weighted imaging, particularly in the TZ (31).

Our study involved multiple readers in a zone-by-zone analysis of the prostate. This was suggested to be more relevant to clinical practice as compared to a region-of-interest analysis (22). Also, our patient cohort consisted of subjects without known prostate malignancy at the time of scan, a few of whom eventually had biopsy-proven prostate malignancy. This approach was chosen to be more reflective of the imaging spectrum in clinical practice given that mpMRI of the prostate is increasingly the first investigation of choice in the initial evaluation of a raised PSA level (32,33).

Our results appear to be mixed when compared to available literature. In our study, combined standard T2 with T2-mapping provided higher Sn and NPV compared to standard T2 alone for detection of prostate malignancy. However, there was trade-off with reduction in Sp. We noted that there is little comparable evidence in the literature and no optimal method on the utilization of

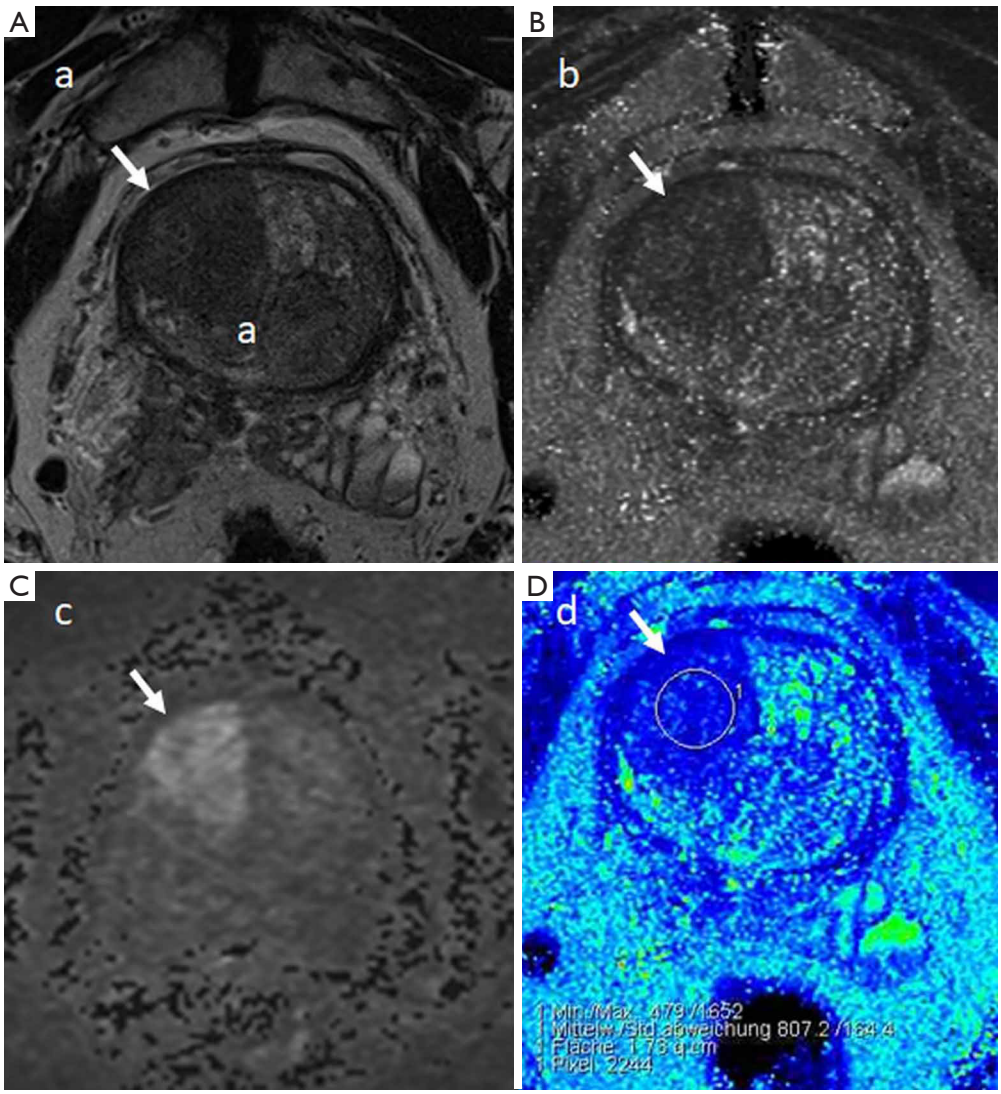

Figure 4 Prostate mpMRI of a 69-year-old gentleman with PSA of 9.3 ng/mL. (A) T2-weighted imaging showed a hypointense lesion with partially-obscured borders in the TZ in the right prostatic lobe (arrow); (B) ADC map showed marked hypointensity (arrow); (C) high b value DWI (b=1,400) showed corresponding marked hyperintensity (arrow). This was given an overall PI-RADS 5 (reference standard positive for malignancy). Also, in this case, targeted biopsy performed after MRI showed Gleason 5+5 prostate cancer; (D) T2-mapping showed a T2-relaxation time of 80.7 ms, below threshold value of 99 ms (arrow). Readers R1 and R2 assigned a T2 PI-RADS score of 3 and both appropriately upgraded to a Likert score of 5 based on combined T2 and T2-mapping. No intravenous contrast was administered in this patient. mpMRI, multiparametric magnetic resonance imaging; PSA, prostate-specific antigen; TZ, transition zone; ADC, apparent diffusion coefficient; DWI, diffusion-weighted imaging.

T2-mapping with standard mpMRI sequences. Wu *et al.* compared diagnostic performance of T2-weighted imaging and T2-star-mapping and found that the combination of T2-weighted imaging and T2-star-mapping provided a significantly higher AUROC, Sn, Sp and accuracy compared to T2-weighted imaging alone (22). However, the method of utilizing the T2-star-maps in that study was not clear. Chatterjee *et al.* found no significant differences in the sensitivities and specificities between T2-weighted imaging and T2-mapping although a significantly higher PPV for T2-mapping was noted (23). However, it was not clear in that study, if the T2-maps were utilized alone or in

conjunction with T2-weighted imaging. Most importantly, the patient cohort in these two studies was biased in favor of prostate malignancy as all patients had histologically-proven prostate malignancy and had undergone radical prostatectomy. One possible explanation for the reduction in Sp for combined standard T2 and T2-mapping in our study could be due to the fact that DWI and DCE imaging, which have been shown to increase Sp compared to T2-weighted imaging alone, were not made available to the readers (34). Although this might limit the applicability in actual clinical practice, this approach was adopted to allow uniform comparison between standard T2 and T2-mapping, and also because it has not been established how T2-mapping complements mpMRI in clinical practice.

In our study, T2-mapping was most accurate when used to re-assess lesions that were deemed of intermediate probability of malignancy on standard T2 (T2 PI-RADS score 3). For lesions that were already classified on standard T2 as low probability of malignancy (T2 PI-RADS score 1 or 2) or high probability of malignancy (T2 PI-RADS score 4 or 5), the addition of T2-mapping was not helpful. Given that the PI-RADS version 2 grading of TZ lesions relies heavily on T2-weighted imaging, T2-mapping could be useful in distinguishing malignancy for PI-RADS 3 lesions in the TZ, and this appears to be supported by our review of the TZs in our study which were assigned a T2 PI-RADS score of 3. However, in our patient cohort there were too few zones in the TZ assigned an overall PI-RADS score of 4 or 5 (6/40 zones), therefore we were not able to perform a meaningful statistical analysis. This reflects the fact that the majority of prostate malignancies occur in the PZ (35). The difficulty in evaluating the usefulness of T2-mapping for TZ malignancies due to the relatively low incidence was also highlighted in other studies (28,36,37).

We observed substantial interobserver variability in analyzing the combined standard T2 with T2-mapping, as evidenced by only "fair" agreement between readers. This suggests that while quantitative measurements should help increase objectivity in imaging analysis, different readers may utilize the parametric T2-maps in combination with T2-weighted imaging differently, with some preferring to place greater emphasis on the T2 and some preferring to place greater emphasis on measured tissue T2-relaxation times from T2-mapping.

Our study has several limitations. First, not all the subjects in our patient cohort eventually had biopsy or proven prostate malignancy. In the study cohort, only 14 out of 40 subjects underwent prostate biopsy. Therefore, we adopted a cumulative reference standard of expert-assigned overall PI-RADS score (taking into account DWI and DCE imaging). Reference standard of biopsy or prostatectomy would usually be ideal for correlation of MRI findings. We agree our results might not have been truly validated in our study in terms of histological correlation. Also because of this, we were unable to make a head-to-head comparison between T2-mapping, DWI and DCE imaging, which would have been ideal. However, biopsy and MRI findings might not always correlate due to either inconsistencies in sample labelling, sampling error or inherent limitations of MRI (38). This can be difficult to determine without analysis of whole-mount prostatectomy specimen. Moreover, in our patient cohort where the majority does not have a prostate malignancy, correlating with histology from prostatectomy would not be practical. Furthermore, our study aimed to evaluate the clinical utility of T2-mapping and how it could potentially be used to complement existing mpMRI sequences, rather than diagnostic accuracy of T2-mapping for cancer detection.

Secondly, whilst our study shows that T2-mapping could be helpful in evaluation of T2 PI-RADS 3 lesions, in current practice this would be relevant only if DWI and/or DCE imaging is non-diagnostic (31). Therefore, excluding reader assessment of DWI and DCE imaging in our study is somewhat artificial and may limit applicability of our study in the clinical setting.

Thirdly, one problem with adopting expert-assigned overall PI-RADS score as reference standard would be the dilemma of PI-RADS 3 scores. Whilst overall PI-RADS scores of 1–2 and 4–5 were reasonably classified as reference standard negative and positive for malignancy, PI-RADS score of 3 was less clear. Given the variable rate of clinically significant malignancy in PI-RADS 3 lesions, ranging from 5–26% (39-41), we therefore classified overall PI-RADS score 3 as reference standard negative for malignancy for purposes of statistical analysis. Similarly, we considered a reader-assigned T2 PI-RADS score of 3 as scan-negative for malignancy, given the relatively low Sn of T2-weighted imaging for prostate cancer detection (42,43). This method of stratification was also performed by Wu *et al.* and Chatterjee *et al.* (22,23).

Finally, the exact lesion locations in our study were not assessed. The location of the reader-identified lesion might not represent that of the reference standard, apart from whether it was located in the PZ or TZ. However, this was to avoid inter-reader ambiguity in definition of the prostatic apex, midgland and base, particularly for small-volume

prostates. Midline lesions might also cause confusion between readers with regards to the laterality (i.e., left or right prostatic lobe). Moreover, there were many subjects with only BPH nodules and identifying a particular nodule in a specific location is usually not clinically relevant in such cases.

In conclusion, quantitative T2-mapping shows potential for improved detection of clinically-significant prostate malignancy, when read in conjunction with T2-weighted imaging. By applying a threshold tissue T2-relaxation time of 99 ms, a combination of T2-weighted imaging and T2-mapping increases Sn and NPV for prostate malignancy compared to T2-weighted imaging alone. T2-mapping was particularly useful in re-categorizing T2 PI-RADS 3 lesions (of intermediate probability of cancer) into either low or high probability of malignancy. However, the application of T2-mapping in conjunction with DWI and DCE imaging as part of mpMRI of the prostate remains uncertain. Further studies are recommended to determine the optimal method of utilizing T2-mapping in clinical practice, and to define its role in complementing established mpMRI sequences.

Acknowledgments

We acknowledge support from the German Research Foundation (DFG) and the Open Access Publication Funds of Charité-Universitätsmedizin Berlin.
Funding: This study has received funding and technical support from Siemens Healthineers.

Footnote

Conflicts of Interest: All authors have completed the ICMJE uniform disclosure form (available at http://dx.doi.org/10.21037/qims-20-222). CHL reports grants and non-financial support from Siemens Healthineers, during the conduct of the study. MT reports grants and non-financial support from Siemens Healthineers, during the conduct of the study; grants and personal fees from CRC 1340/1 (DFG, Germany Research Foundation), outside the submitted work. PA reports grants and non-financial support from Siemens Healthineers, during the conduct of the study; personal fees from b.e.imaging, grants from CRC 1340/1 (DFG, Germany Research Foundation), other from ESR European Society of Radiology, other from DRG Germany Roentgen Society, personal fees and other from CSR Chinese Society of Radiology, outside the submitted work. MH reports grants and non-financial support from Siemens Healthineers, during the conduct of the study; personal fees from b.e.imaging, outside the submitted work. The other author has no conflicts of interest to declare.

Ethical Statement: The study was conducted in accordance with the Declaration of Helsinki (as revised in 2013). This prospective single-center study was approved by the institutional board of Charité University Hospital—Campus Benjamin Franklin (No. EA4/010/16) and informed consent was taken from all the patients. .

References

1. Hegde JV, Mulkern RV, Panych LP, Fennessy FM, Fedorov A, Maier SE, Tempany CM. Multiparametric MRI of prostate cancer: an update on state-of-the-art techniques and their performance in detecting and localizing prostate cancer. J Magn Reson Imaging 2013;37:1035-54.
2. Barentsz JO, Richenberg J, Clements R, Choyke P, Verma S, Villeirs G, Rouviere O, Logager V, Fütterer JJ; European Society of Urogenital Radiology. ESUR prostate MR guidelines 2012. Eur Radiol 2012;22:746-57.
3. Kasivisvanathan V, Rannikko AS, Borghi MN, Panebianco V, Mynderse LA, Vaarala MH, Briganti A, Budäus L, Hellawell G, Hindley RG, Roobol MJ, Eggener S, Ghei M, Villers A, Bladou F, Villeirs GM, Virdi J, Boxler S, Robert G, Singh PB, Venderink W, Hadaschik BA, Ruffion A, Hu JC, Margolis D, Crouzet S, Klotz L, Taneja SS, Pinto P, Gill I, Allen C, Giganti F, Freeman A, Morris S, Punwani S, Williams NR, Brew-Graves C, Deeks J, Takwoingi Y, Emberton M, Moore CM; PRECISION Study Group Collaborators. MRI-targeted or standard biopsy for prostate cancer diagnosis. N Engl J Med 2018;378:1767-77.
4. Ahmed HU, El-Shater BA, Brown LC, Brown LC, Gabe R, Kaplan R, Parmar MK, Collaco-Moraes Y, Ward K, Hindley RG, Freeman A, Kirkham AP, Oldroyd R, Parker C, Emberton M; PROMIS study group.

Diagnostic accuracy of multiparametric MRI and TRUS biopsy in prostate cancer (PROMIS): a paired validating confirmatory study. Lancet 2017;389:815-22.
5. Garmer M, Busch M, Mateiescu S, Fahlbusch DE, Wagener B, Grönemeyer DH. Accuracy of MRI-targeted in-bore prostate biopsy according to the Gleason score with postprostatectomy histopathologic control - a targeted biopsy-only strategy with limited number of cores. Acad Radiol 2015;22:1409-18.
6. Baco E, Rud E, Eri LM, Moen G, Vlatkovic L, Svindland A, Eggesbø HB, Ukimura O. A randomized controlled trial to assess and compare the outcomes of two-core prostate biopsy guided by fused magnetic resonance and transrectal ultrasound images and traditional 12-core systematic biopsy. Eur Urol 2016;69:149-56.
7. Chesnais AL, Niaf E, Bratan F, Mège-Lechevallier F, Roche S, Rabilloud M, Colombel M, Rouvière O. Differentiation of transitional zone prostate cancer from benign hyperplasia nodules: evaluation of discriminant criteria at multiparametric MRI. Clin Radiol 2013;68:e323-30.
8. van Niekerk CG, Witjes JA, Barentsz JO, van der Laak JAWM, Hulsbergen-van der Kaa CA. Microvascularity in transition zone prostate tumors resembles normal prostatic tissue. Prostate 2013;73:467-75.
9. Shinmoto H, Tamura C, Soga S, Shiomi E, Yoshihara N, Kaji T, Mulkern RV. An intravoxel incoherent motion diffusion-weighted imaging study of prostate cancer. AJR Am J Roentgenol 2012;199:W496-500.
10. Gürses B, Tasdelen N, Yencilek F, Kılıckesmez NO, Alp T, Fırat Z, Albayrak MS, Uluğ AM, Gürmen AN. Diagnostic utility of DTI in prostate cancer. Eur J Radiol 2011;79:172-6.
11. Tamura C, Shinmoto H, Soga S, Okamura T, Sato H, Okuaki T, Pang Y, Kosuda S, Kaji T. Diffusion kurtosis imaging study of prostate cancer: preliminary findings. J Magn Reson Imaging 2014;40:723-9.
12. Sabouri S, Chang SD, Savdie R, Zhang J, Jones EC, Goldenberg SL, Black PC, Kozlowski P. Luminal Water Imaging: a new MRI T2 mapping technique for prostate cancer diagnosis. Radiology 2017;284:451-9.
13. Gilani N, Rosenkrantz AB, Malcolm P, Johnson G. Minimization of errors in biexponential T2 measurements of the prostate. J Magn Reson Imaging 2015;42:1072-7.
14. Kim PK, Hong YJ, Im DJ, Suh YJ, Park CH, Kim JY, Chang S, Lee HJ, Hur J, Kim YJ, Choi BW. Myocardial T1 and T2 mapping: techniques and clinical applications. Korean J Radiol 2017;18:113-31.
15. Knight MJ, McCann B, Tsivos D, Dillon S, Coulthard E, Kauppinen RA. Quantitative T2 mapping of white matter: applications for ageing and cognitive decline. Phys Med Biol 2016;61:5587-605.
16. Mamisch TC, Trattnig S, Quirbach S, Marlovits S, White LM, Welsch GH. Quantitative T2 mapping of knee cartilage: differentiation of healthy control cartilage and cartilage repair tissue in the knee with unloading - initial results. Radiology 2010;254:818-26.
17. Hoang Dinh A, Souchon R, Melodelima C, Bratan F, Mège-Lechevallier F, Colombel M, Rouvière O. Characterization of prostate cancer using T2 mapping at 3T: a multiscanner study. Diagn Interv Imaging 2015;96:365-72.
18. Liu W, Turkbey B, Senegas J, Remmele S, Xu S, Kruecker J, Bernardo M, Wood BJ, Pinto PA, Choyke PL. Accelerated T2 mapping for characterization of prostate cancer. Magn Reson Med 2011;65:1400-6.
19. Yamauchi FI, Penzkofer T, Fedorov A, Fennessy FM, Chu R, Maier SE, Tempany CM, Mulkern RV, Panych LP. Prostate cancer discrimation in the peripheral zone with a reduced field-of-view T2-mapping MRI sequence. Magn Reson Imaging 2015;33:525-30.
20. Sumpf TJ, Uecker M, Boretius S, Frahm J. Model-based nonlinear inverse reconstruction for T2 mapping using highly undersampled spin-echo MRI. J Magn Reson Imaging 2011;34:420-8.
21. Weinreb JC, Barentsz JO, Choyke PL, Cornud F, Haider MA, Macura KJ, Margolis D, Schnall MD, Shtern F, Tempany CM, Thoeny HC, Verma S. PI-RADS prostate imaging - reporting and data system: 2015, version 2. Eur Urol 2016;69:16-40.
22. Wu LM, Yao QY, Zhu J, Lu Q, Suo ST, Liu Q, Xu JR, Chen XX, Haacke EM, Hu J. T2* mapping combined with conventional T2-weighted image for prostate cancer detection at 3.0T MRI: a multi-observer study. Acta Radiol 2017;58:114-20.
23. Chatterjee A, Devaraj A, Mathew M, Szasz T, Antic T, Karczmar GS, Oto A. Performance of T2 maps in the detection of prostate cancer. Acad Radiol 2019;26:15-21.
24. Garcia-Reyes K, Passoni NM, Palmeri ML, Kauffman CR, Choudhury KR, Polascik TJ, Gupta RT. Detection of prostate cancer with multiparametric MRI (mpMRI): effect of dedicated reader education on accuracy and confidence of index and anterior cancer diagnosis. Abdom Imaging 2015;40:134-42.
25. Ruprecht O, Weisser P, Bodelle B, Ackermann H, Vogl TJ. MRI of the prostate: interobserver agreement compared with histopathologic outcome after radical prostatectomy.

Eur J Radiol 2012;81:456-60.
26. Metzger GJ, Kalavagunta C, Spilseth B, Bolan PJ, Li X, Hutter D, Nam JW, Johnson AD, Henriksen JC, Moench L, Konety B, Warlick CA, Schmechel SC, Koopmeiners JS. Detection of prostate cancer: quantitative multiparameteric MR imaging models developed using registered correlative histopathology. Radiology 2016;279:805-16.
27. van Houdt PJ, Agarwal HK, van Buuren LD, Heijmink SWTPJ, Haack S, van der Poel HG, Ghobadi G, Pos FJ, Peeters JM, Choyke PL, van der Heide UA. Performance of a fast and high-resolution multi-echo spin-echo sequence for prostate T2 mapping across multiple systems. Magn Reson Med 2018;79:1586-94.
28. Langer DL, van der Kwast TH, Evans AJ, Plotkin A, Trachtenberg J, Wilson BC, Haider MA. Prostate tissue composition and MR measurements: investigating the relationships between ADC, T2, K(trans), v(e), and corresponding histologic features. Radiology 2010;255:485-94.
29. Dregely I, Margolis DA, Sung K, Zhou Z, Rangwala N, Raman SS, Wu HH. Rapid quantitative T2 mapping of the prostate using three-dimensional dual echo steady state MRI at 3T. Magn Reson Med 2016;76:1720-9.
30. Gibbs P, Tozer DJ, Liney GP, Turnbull LW. Comparison of quantitative T2 mapping and diffusion-weighted imaging in the normal and pathologic prostate. Magn Reson Med 2001;46:1054-8.
31. Purysko AS, Rosenkrantz AB, Barentsz JO, Weinreb JC, Macura KJ. PI-RADS Version 2: A pictorial update. RadioGraphics 2016;36:1354-72.
32. Wang R, Wang J, Gao G, Hu J, Jiang Y, Zhao Z, Zhang X, Zhang YD, Wang X. Prebiopsy mp-MRI can help to improve the predictive performance in prostate cancer: a prospective study in 1,478 consecutive patients. Clin Cancer Res 2017;23:3692-9.
33. Haffner J, Lemaitre L, Puech P, Haber GP, Leroy X, Jones JS, Villers A. Role of magnetic resonance imaging before initial biopsy: comparison of magnetic resonance imaging-targeted and systematic biopsy for significant prostate cancer detection. BJU Int 2011;108:E171-8.
34. Fusco R, Sansone M, Granata V, Setola SV, Petrillo A. A systematic review on multiparametric MR imaging in prostate cancer detection. Infect Agents Cancer 2017;12:57.
35. Patel V, Merrick GS, Allen ZA, Andreini H, Taubenslag W, Singh S, Butler WM, Adamovich E, Bittner N. The incidence of transition zone prostate cancer diagnosed by transperineal template-guided mapping biopsy: implications for treatment planning. Urology 2011;77:1148-52.
36. Foltz WD, Chopra S, Chung P, Bayley A, Catton C, Jaffray D, Wright GA, Haider MA, Ménard C. Clinical prostate T2 quantification using magnetization-prepared spiral imaging. Magn Reson Med 2010;64:1155-61.
37. Giganti F, Gambarota G, Moore CM, Robertson NL, McCartan N, Jameson C, Bott SRJ, Winkler M, Whitcher B, Castro-Santamaria R, Emberton M, Allen C, Kirkham A. Prostate cancer detection using quantitative T2 and T2 -weighted imaging: the effects of 5-alpha-reductase inhibitors in men on active surveillance. J Magn Reson Imaging 2018;47:1646-53.
38. Rosenkrantz AB, Deng FM, Kim S, Lim RP, Hindman N, Mussi TC, Spieler B, Oaks J, Babb JS, Melamed J, Taneja SS. Prostate cancer: multiparametric MRI for index lesion localization—a multiple-reader study. AJR Am J Roentgenol 2012;199:830-7.
39. Pokorny MR, de Rooij M, Duncan E, Schröder FH, Parkinson R, Barentsz JO, Thompson LC. Prospective study of diagnostic accuracy comparing prostate cancer detection by transrectal ultrasound-guided biopsy 8 versus magnetic resonance (MR) imaging with subsequent MR-guided biopsy in men without previous prostate biopsies. Eur Urol 2014;66:22-9.
40. Thompson J, Lawrentschuk N, Frydenberg M, Thompson L, Stricker P. The role of magnetic resonance imaging in the diagnosis and management of prostate cancer. BJU Int 2013;112 Suppl 2:6-20.
41. Liddell H, Jyoti R, Haxhimolla HZ. Mp-MRI Prostate characterised PIRADS 3 lesions are associated with a low risk of clinically significant prostate cancer - a retrospective review of 92 biopsied PIRADS 3 lesions. Curr Urol 2015;8:96-100.
42. Gaur S, Harmon S, Gupta RT, Margolis DJ, Lay N, Mehralivand S, Merino MJ, Wood BJ, Pinto PA, Shih JH, Choyke PL, Turkbey B. A multireader exploratory evaluation of individual pulse sequence cancer detection on prostate multiparametric magnetic resonance imaging (MRI). Acad Radiol 2019;26:5-14.
43. Tan CH, Wei W, Johnson V, Kundra V. Diffusion-weighted MRI in the detection of prostate cancer: meta-analysis. AJR Am J Roentgenol 2012;199:822-9.

Cite this article as: Lee CH, Taupitz M, Asbach P, Lenk J, Haas M. Clinical utility of combined T2-weighted imaging and T2-mapping in the detection of prostate cancer: a multi-observer study. Quant Imaging Med Surg 2020;10(9):1811-1822. doi: 10.21037/qims-20-222

